Columnar Liquid Crystalline Glasses by Combining Configurational Flexibility with Moderate Deviation from Planarity: Extended Triaryltriazines

Fabrícia Nunes da Silva, Hugo Marchi Luciano, Carlos Stadtlober, Giliandro Farias, Fabien Durola, Juliana Eccher, Ivan Bechtold, Harald Bock, Hugo Gallardo, André Vieira

Columnar Liquid Crystalline Glasses by Combining Configurational Flexibility with Moderate Deviation from Planarity: Extended Triaryltriazines

Fabrícia Nunes da Silva,[a, b] Hugo Marchi Luciano,[b, c] Carlos H. Stadtlober,[d] Giliandro Farias,[c] Fabien Durola,[e] Juliana Eccher,[d] Ivan H. Bechtold,*[d] Harald Bock,*[e] Hugo Gallardo,[c] and André A. Vieira*[a]

Abstract: Triply phenanthryl- and tetrahelicenyl-substituted triazine-hexaalkyl esters with short alkyl chains show glass transitions conveniently above room temperature within the hexagonal columnar liquid crystalline state, resulting in a solid columnar order at room temperature. As the hexagonal columnar mesophase is easily aligned with the director perpendicular to a solid substrate, such glassy columnar liquid matrices are aimed at for the orientation of guest emitters, to obtain anisotropic emission. A condition for face-on alignment on substrates are attainable melting and clearing temperatures, which is achieved with the moderately nonplanar tetrahelicenyl derivatives in spite of their short alkyl periphery. An unusual phase transition between two columnar mesophases of same hexagonal symmetry, but very different long-distance regularity of the column lattice, is found in one phenanthryl homolog.

Introduction

Glassy polyaromatic matrices are widespread in organic electronics, because use of the glass state circumvents the electric (such as inhomogeneous charge transport, trap pinning) and optical (such as scattering) problems arising from grain boundaries in microcrystalline materials, whilst still providing the mechanical robustness of a solid. The formation of glasses instead of crystals is favored by conformational multiplicity and the presence of dipoles. Whilst isotropic glasses are common amongst charge-transporting polycyclic aromatics, liquid crystalline polyaromatic glasses are much rarer. They allow embedding of emitter materials in an oriented anisotropic alignment, favoring anisotropic emission, which can lead to a 50% increase of light outcoupling and thus of external device efficiency.[1] Hexagonal columnar liquid crystals are especially interesting, as they tend to align homeotropically (i.e. with the disk-shaped molecules parallel to the substrate),[2] favoring an emitter orientation with preferred emission perpendicular to the device plane.

Columnar liquid crystals generally consist of molecules that have a more or less rigid polycyclic aromatic core with a flexible alkyl chain periphery.[3] Besides rarer cases of nematic mesophases that lack periodic order,[4] such disk-like mesogens form columnar stacks of disks, and the columns form a two-dimensional ordered lattice, whilst no long-range order persists in the direction of the column axes. Different columnar mesophases with different symmetries of the column lattice exist, the most common being hexagonal symmetry, which generally results if the disk planes are on average perpendicular to the column axis. Mesophases of rectangular or oblique symmetry result mainly from slipped stacking, which makes the disks tilt out of the plane normal to the column axis, and leads to a non-circular column cross-section. The close disk-to-disk stacking leads to generally good charge and exciton transport along the columns.[5] The formation of a glassy columnar liquid crystalline state close to room temperature by non-polymeric discotic mesogens has been observed previously mainly in dimeric systems like bridged hexaalkoxy-triphenylene dimers;[6] another design approach relies on monomeric mesogens with heavy anchor-like side-chains, where crystallization may additionally be impeded by low symmetry or regio-isomer mixing (Scheme 1).[7]

[a] *F. Nunes da Silva, Prof. A. A. Vieira*
Departamento de Química
Universidade Federal da Bahia
Ondina, 40170-115 Salvador, BA (Brazil)
E-mail: vieira.andre@ufba.br

[b] *F. Nunes da Silva, H. Marchi Luciano*
Centre de Recherche Paul Pascal
Université Bordeaux
115 av. Schweitzer, 33600 Pessac (France)

[c] *H. Marchi Luciano, Dr. G. Farias, Prof. H. Gallardo*
Departamento de Química
Universidade Federal de Santa Catarina
Trindade, 88040-900 Florianópolis, SC (Brazil)

[d] *C. H. Stadtlober, Prof. J. Eccher, Prof. I. H. Bechtold*
Departamento de Física
Universidade Federal de Santa Catarina
Trindade, 88040-900 Florianópolis, SC (Brazil)
E-mail: ivan.bechtold@ufsc.br

[e] *Dr. F. Durola, Dr. H. Bock*
Centre de Recherche Paul Pascal, CNRS
115 av. Schweitzer, 33600 Pessac (France)
E-mail: harald.bock@crpp.cnrs.fr

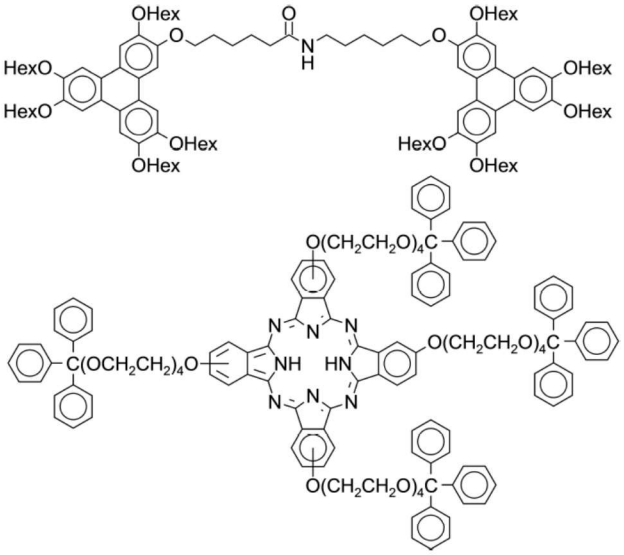

Scheme 1. Examples of known glass forming columnar mesogens with conventional triphenylene or phthalocyanine cores: spacer-bridged dimer (top) and monomeric disc with bulky substituents (bottom); Hex = *n*-hexyl.

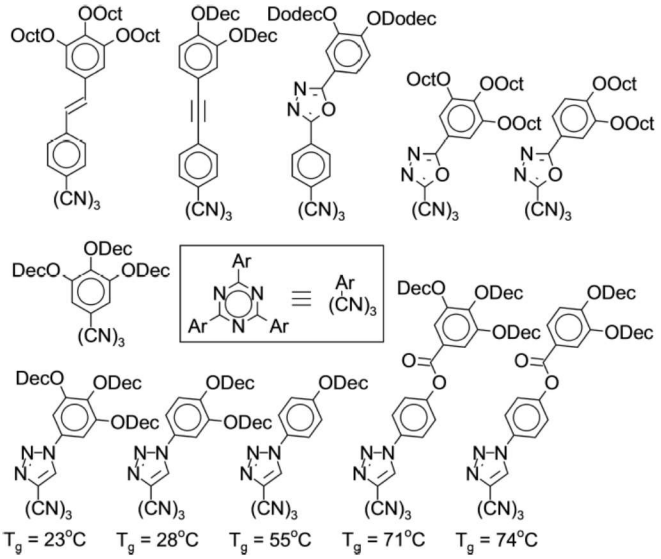

Scheme 2. Examples of known columnar triaryltriazine mesogens with three to nine alkoxy chains; Hex = *n*-hexyl, Dec = *n*-decyl, Dodec = *n*-dodecyl.[9] The bottom row shows materials where a glass transition above room temperature in the columnar mesophase has been observed by calorimetry (T_g given).

It has recently been shown that both the alignment direction and the entropy content (disorder) of a small molecule room temperature columnar liquid crystalline glass can be controlled during physical vapor deposition by the adjustment of deposition speed and substrate temperature.[8] Such procedures rely on sublimable mesogens of small molecular weight.

A simple heterocyclic structural motif with threefold symmetry that has been reported to yield predominantly hexagonal columnar mesophases when appropriately extended with alkoxy-decorated aryl substituents is 1,3,5-triazine.[9] Most of these columnar triaryltriazines have rather large molecular weights because the alkoxy chains needed to induce mesomorphism are long and come in large number. In several tris(triazolyl)triazine derivatives, calorimetric glass transitions above room temperature could be detected after melting and subsequent cooling, confirming the presence of an anisotropic columnar glass at standard conditions (Scheme 2).

We recently reported that ester-substituted triphenyltriazines, i.e. tris(3-alkoxycarbonylphenyl)-*s*-triazines **1**, (Scheme 3) can be obtained swiftly from methyl 3-cyanobenzoate in analogy to the acid-induced trimerization of benzonitrile,[10] and predominantly show nematic liquid crystal behavior.[11] Core- or chain-fluorination leads to columnar mesophases with only weak tendency to crystallize at room temperature, due to the rotational flexibility at the triazine-benzene single bond that allows for two in-plane configurations of each meta-attached ester group with respect to this bond. The limited conjugation between the three outer benzene units via meta-linkages through the central triazine cycle ensures that a large band gap is preserved, allowing for the embedding of blue emitters, as is desired eg. for TADF (thermally activated delayed fluorescence) OLEDs (organic light emitting diodes).[12] Unfortunately, we could not obtain a robust glassy state in a convenient temperature range above room temperature with these smallest representatives of the triaryltriazine esters.

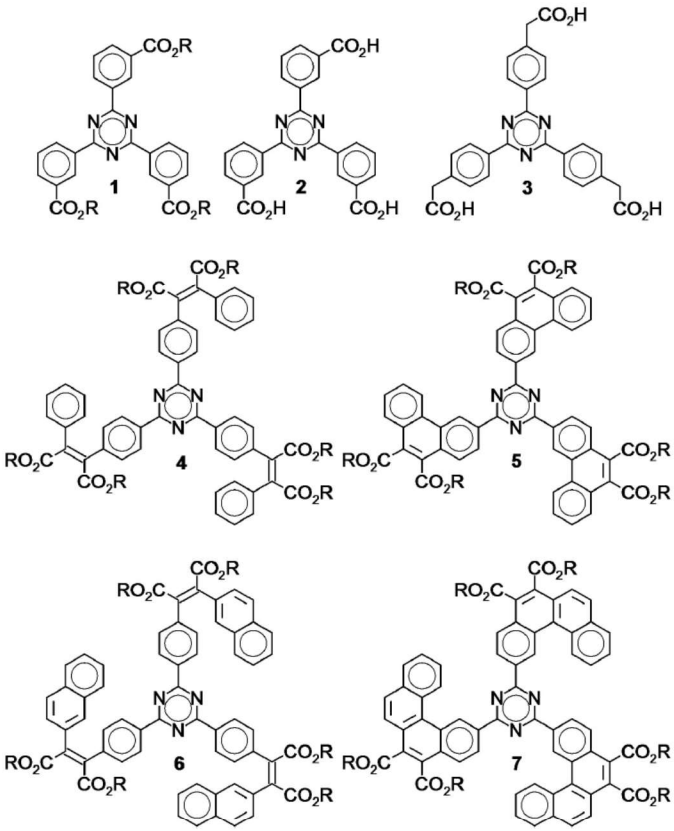

Scheme 3. Liquid crystalline triaryltriazine hexaesters and their synthetic precursors.

Table 1. Calorimetric phase transition onset temperatures (°C) and enthalpies (J/g [in brackets]), and glass transition onset temperatures, on heating with 10 °C/min; Cr = crystalline phase, Col_{hex} = hexagonal columnar mesophase, Iso = isotropic liquid, T_g = glass transition temperature in the hexagonal columnar mesophase (Col) or in the isotropic liquid (Iso); monotropic transitions (observed on second heating only, after cooling from the isotropic liquid) in italics. The two right-hand columns give the column-to-column distance d_{col} and the intracolumnar disk stacking distance d_{disk} in Å at 25 °C in the hexagonal mesophase, as observed by powder XRD.

	Cr–Cr	Cr–Col_{hex}	Col_{hex}–Col_{hex}	Col_{hex}-Iso	Cr-Iso	T_g	d_{col}	d_{disk}
$\mathbf{5}_{Et}$	224[26]				>375			
$\mathbf{5}_{Pr}$		150[13]		>375		*81*^{Col}	20.8	-
$\mathbf{5}_{Bu}$		108[11]		>375		*19*^{Col}	23.5	3.3
$\mathbf{7}_{Et}$	153[12]				325[26]			
$\mathbf{7}_{Pr}$			*179 [1.9]*	*223[3.0]*	232[37]		22.2	3.7
$\mathbf{7}_{Bu}$				*149[1.0]*	205[34]	*39*^{Col}	22.5	3.7
$\mathbf{7}_{Hex}$					123[22]	*27*^{Iso}		

The glyoxylic Perkin reaction,[13] combined with subsequent Mallory photocyclization, is a versatile tool for the synthesis of polycyclic arenes with multiple viscosity-enhancing alkyl ester substituents, and such ester substituents often lead to liquid crystalline materials even when only very short alkyl peripheries are used.[14]

Whilst the trimerization of 3-cyanobenzoic acid, in contrast to the successful trimerization of its methyl ester, to the corresponding tricarboxy-triphenyltriazine **2** (Scheme 3) is accompanied by substantial degradation, we now found that (4-cyanophenyl)acetic acid trimerizes cleanly, yielding a convenient substrate for threefold Perkin-Mallory sequences that allow the synthesis of extended triaryltriazine hexaesters. When the so-obtained trimer, tris((4-carboxymethyl)phenyl)triazine **3**, is Perkin-condensed with phenylglyoxylic acid, and the resulting tris(maleic acid) $\mathbf{4}_H$ is subjected to in situ esterification and subsequent Mallory photocyclization, triphenanthryl-triazines **5** bearing three pairs of vicinal ester substituents are obtained.

The alkyl groups introduced by in situ esterification should be short enough to allow a glassy state at room temperature (avoiding undue fluidification), but sufficiently long to allow mesophase formation. Methyl ester groups rarely allow the latter, whereas in many systems, already ethyl ester groups do. Whilst a high glass transition temperature T_g is desirable to ensure solid-like robustness well above room temperature, an attainable clearing temperature well below the temperatures of thermal degradation of organic materials (that are typically around 300 °C) is also desirable to allow cooling trough the liquid-to-mesophase transition (a.k.a. clearing temperature T_{cl}) as a means of homogeneously aligning the mesophase's optical axis with respect to the substrate.

We thus prepared the hexaethyl, hexapropyl and hexabutyl ester derivatives $\mathbf{5}_{Et}$, $\mathbf{5}_{Pr}$ and $\mathbf{5}_{Bu}$ of sym-tris(phenanthr-3-yl)triazine.

Results and Discussion

Albeit the hexaethyl ester $\mathbf{5}_{Et}$ shows, as confirmed by powder Xray diffraction (XRD), a phase transition between two different crystalline states upon heating above its melting onset at 224 °C, no transition to the isotropic liquid is observable by polarized light optical microscopy (POM) up to our experimental limit of 375 °C. The propyl homolog $\mathbf{5}_{Pr}$, after melting at 150 °C, (Table 1) likewise shows no clearing to the isotropic liquid below 375 °C, but the high temperature state is identified as a hexagonal columnar mesophase (by the characteristic (11) and (21) secondary XRD peaks of the column lattice corresponding to distances related by factors of $\sqrt{3}$ and $\sqrt{7}$ to the main lattice peak)[15] (Figure 1), which upon cooling to room temperature rigidifies to a non-shearable mesomorphic glass. The XRD spectra of $\mathbf{5}_{Pr}$ at 250 and 25 °C testify of a contraction of 10 % of the column-to-column distances (from 23.0 Å to 20.7 Å) over this temperature span, accompanied by roughening of the

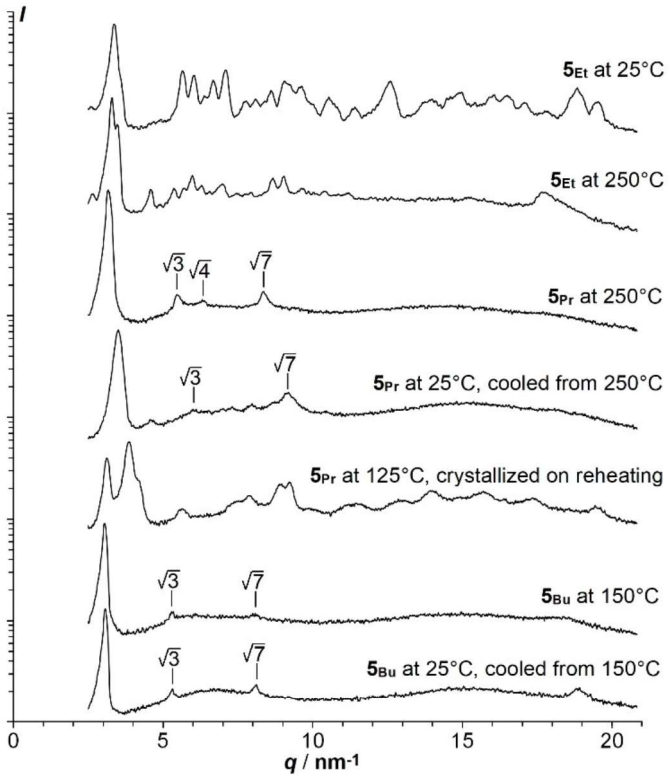

Figure 1. Powder XRD spectra of $\mathbf{5}_{Et}$, $\mathbf{5}_{Pr}$ and $\mathbf{5}_{Bu}$ at room and elevated temperature (logarithmic intensity scaling). The root values indicate the q ratio with the main lattice peak to the left and correspond to a column lattice of hexagonal symmetry; the corresponding Miller indices are $\sqrt{3}$: (11), $\sqrt{4}$: (20), $\sqrt{7}$: (21).

diffraction pattern in the small angle region, but without loss of the (11) and (21) peaks.

A steplike feature is apparent in the calorimetric cooling curve of $\mathbf{5}_{Pr}$ between 85 and 63 °C (at −10 °C/min), (Figure 2) whereas a similar feature above 81 °C on the corresponding heating curve (at +10 °C/min, calorimetric glass transition temperatures are most commonly recorded upon heating at that speed) is convoluted with heating-induced crystallization between 100 and 130 °C. A calorimetric glass transition on heating thus cannot clearly be distinguished, but shearing of the mesophase between glass slides at temperatures below 81 °C is impossible, corroborating the formation of a mesomorphic glass. The inferred glass transition at ca. 81 °C restricts crystallization to the temperature domain between this temperature and the melting onset at 150 °C. In the butyl homolog $\mathbf{5}_{Bu}$, which likewise shows a hexagonal columnar mesophase after melting at 108 °C, the calorimetric glass transition is significantly lowered to 19 °C, whereas, in contrast to $\mathbf{5}_{Pr}$, immediate crystallization upon heating above this glass transition is not observed. Like its two smaller homologs, $\mathbf{5}_{Bu}$ does not clear below 375 °C. The hexagonal lattice parameter of $\mathbf{5}_{Bu}$ is preserved by cooling from 150 °C to room temperature, with a column-to-column distance of 23.5 Å that shows no significant temperature dependence. The π-stacking order inside the columns, corresponding to an interdisk distance of about 3.3 Å, was enhanced upon cooling to room temperature, which facilitates charge carrier transport. In contrast, the π-stacking order was not clearly observed for $\mathbf{5}_{Pr}$, neither at high nor at room temperature.

Even though we were able to obtain with $\mathbf{5}_{Pr}$ a mesomorphic anisotropic glass with a conveniently high glass transition temperature of 81 °C, the absence of clearing to the isotropic liquid at practical temperatures and the drop of the glass transition temperature to only 19 °C with $\mathbf{5}_{Bu}$ led us to redesign the molecular structure.

Extension of the three aryl arms with 2-naphthylglyoxylic acid via the Perkin adduct $\mathbf{6}_{H}$ to target esters **7** with off-planar tetrahelicenyl units[16] offered the perspective of both lowering the clearing temperature due to a less planar and relatively compact molecular shape and hindering the tendency to crystallize due to increased conformational variations, both in-plane and out-of-plane.

We thus prepared analogously the hexaethyl, hexapropyl and hexabutyl ester derivatives $\mathbf{7}_{Et}$, $\mathbf{7}_{Pr}$ and $\mathbf{7}_{Bu}$ of sym-tris(tetrahelicen-3-yl)triazine. All three homologs show direct melting of the crystalline state to the isotropic liquid at attainable temperatures of 325, 232 and 205 °C, respectively. No mesophase is detected with $\mathbf{7}_{Et}$ on cooling from the isotropic liquid, and a crystal-to-crystal transition is observed by DSC (at 153 °C on heating). Both crystalline phases are of hexagonal symmetry, showing the characteristic (10), (11), (20), (21), (30), (22) and (31) peaks corresponding to hexagonal lattice distances in the ratios of $1:\sqrt{3}:\sqrt{4}:\sqrt{7}:\sqrt{9}:\sqrt{12}:\sqrt{13}$, besides a multitude of other peaks (Figure 3). In contrast to $\mathbf{7}_{Et}$, the crystalline phases of $\mathbf{7}_{Pr}$ and $\mathbf{7}_{Bu}$ do not show prominent XRD peaks associable with a hexagonal lattice. $\mathbf{7}_{Pr}$ and $\mathbf{7}_{Bu}$ show monotropic mesophases upon cooling below their clearing points at 223 and 149 °C, respectively, with the typical growth textures of the hexagonal columnar mesophase (Figure 4) and

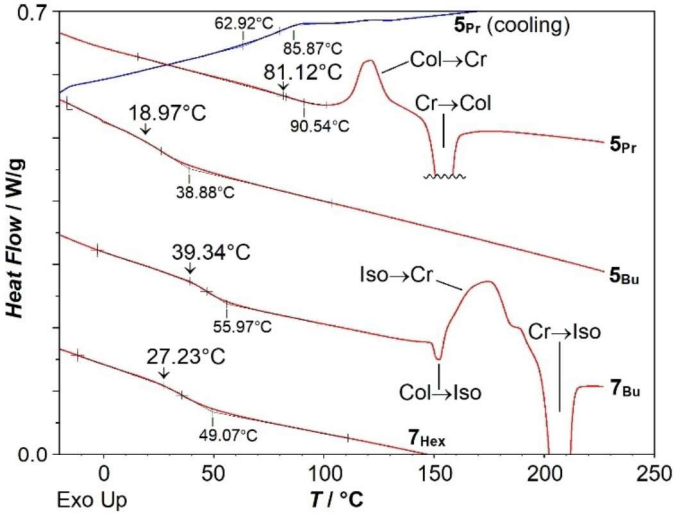

Figure 2. Differential calorimetry heating scans (red) of $\mathbf{5}_{Pr}$, $\mathbf{7}_{Bu}$, $\mathbf{7}_{Bu}$ and $\mathbf{7}_{Hex}$ at +10 °C/min (after initial heating above the melting point and subsequent cooling at −10 °C/min), and cooling scan (blue) of $\mathbf{5}_{Pr}$ at −10 °C/min; glass transition onset temperatures on heating are indicated above vertical arrows; phase transitions are marked between Col = hexagonal columnar mesophase, Cr = crystalline state, and Iso = isotropic liquid.

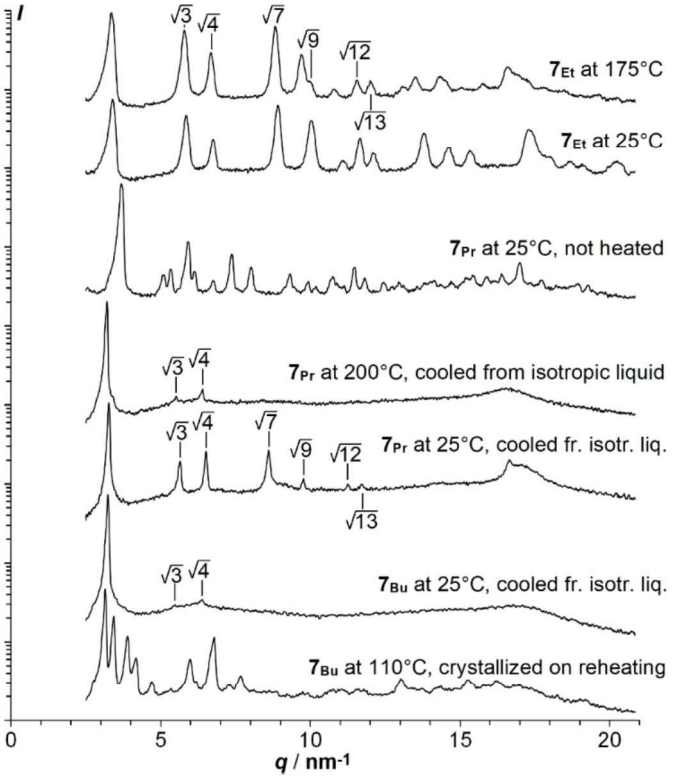

Figure 3. Powder XRD spectra of $\mathbf{7}_{Et}$, $\mathbf{7}_{Pr}$ and $\mathbf{7}_{Bu}$ at room and elevated temperature (logarithmic intensity scaling). The root values indicate the q ratio with the main lattice peak to the left and correspond to a column lattice of hexagonal symmetry; the corresponding Miller indices are √3: (11), √4: (20), √7: (21), √9: (30), √12: (22), √13: (31).

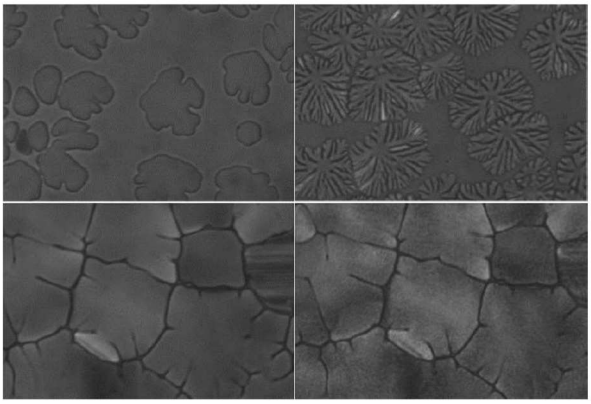

Figure 4. Growth between glass plates of the hexagonal columnar mesophase of $\mathbf{7}_{Pr}$ (top left) and $\mathbf{7}_{Bu}$ (top right) in homeotropic alignment upon cooling through the isotropic-columnar phase transition, and homeotropic texture of the high temperature mesophase of $\mathbf{7}_{Pr}$ at 200 °C (bottom left) and of the low temperature mesophase at 100 °C (bottom right) after cooling from the isoptropic liquid followed by reheating; polarizing light optical microcopy with slightly uncrossed polarizers.

associated $\sqrt{3}$ and $\sqrt{4}$ XRD peaks. Thus, the slight deplanarization of the aromatic core destabilizes the hexagonal mesophase sufficiently to deliver attainable clearing temperatures in $\mathbf{7}_{Pr}$ and $\mathbf{7}_{Bu}$, whilst the mesophase is entirely suppressed in $\mathbf{7}_{Et}$ in favor of a hexagonal crystal. Upon cooling, $\mathbf{7}_{Pr}$ shows a further low-enthalpy transition that is unique to this compound and that is significantly hysteretic with onset temperatures on cooling and reheating with 10 °C/min of 143 and 179 °C, respectively (Figure 5). Astonishingly, this transition reveals itself by XRD to be associated with no change of the hexagonal symmetry of the mesophase and no appearance of peaks not associable with a 2D hexagonal lattice, but the higher order peaks of the column lattice increase significantly in relative intensity with respect to the primary lattice peak (and the $\sqrt{7}$, $\sqrt{9}$, $\sqrt{12}$ and $\sqrt{13}$ peaks are now clearly expressed). Thus, XRD testifies of an improved correlation length of the column lattice and an enhancement of the interdisk peak. Similar to $\mathbf{5}_{Pr}$, a slight contraction of the column-to-column distance (from 22.6 Å at 200 °C to 22.2 Å at 25 °C) and of the π-stacking distance (from 3.8 Å to 3.7 Å) was also observed for $\mathbf{7}_{Pr}$. No

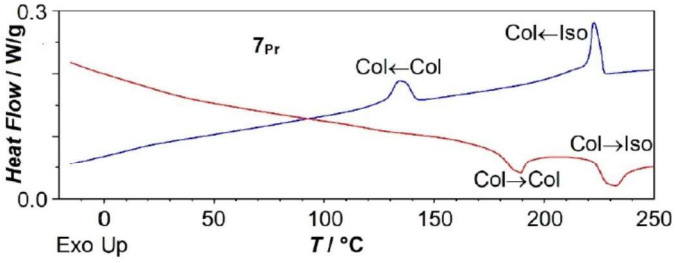

Figure 5. Differential calorimetry cooling (blue) and subsequent heating (red) scans of $\mathbf{7}_{Pr}$ at −/+ 10 °C/min (after initial heating above the melting point); with phase transitions between two hexagonal columnar (Col) mesophases and between the higher temperature mesophase and the isotropic liquid (Iso).

calorimetric glass transition could be observed with $\mathbf{7}_{Pr}$ within the temperature range of this highly ordered mesophase.

When $\mathbf{7}_{Pr}$ is sandwiched between glass slides in homeotropic alignment, the transition between the two hexagonal phases manifests itself in the microscope by a reversible increase of granularity, without change of domain boundaries (Figure 4).

No such less-to-more-regular-mesophase transition is observed with $\mathbf{7}_{Bu}$, but it forms a mesomorphic glass at room temperature and shows a calorimetric glass transition at 39 °C on reheating (+10 °C/min). Thus, $\mathbf{7}_{Bu}$ shows both a persistent mesomorphic hexagonal columnar glass at room temperature (with column-to-column distance of 22.5 Å and intercolumnar distance of 3.7 Å) and conveniently accessible melting and clearing temperatures of 205 and 149 °C.

To evaluate whether slightly longer alkyl chains on **7** would still allow a mesomorphic glass at room temperature, we also prepared the homolog $\mathbf{7}_{Hex}$ with n-hexyl ester substituents, and we were surprised to find that it is not mesogenic but forms an isotropic glass (T_g = 27 °C on heating at +10 °C/min) after melting at 123 °C and cooling back to room temperature.

Thus, a hexagonal columnar mesophase was observed with the four materials $\mathbf{5}_{Pr}$, $\mathbf{5}_{Bu}$, $\mathbf{7}_{Pr}$ and $\mathbf{7}_{Bu}$, of which $\mathbf{7}_{Pr}$ shows a peculiar thermal phase transition between two distinct hexagonal states with different degrees of order of the column lattice. No mesophase was observed with either shorter ethyl chains in $\mathbf{5}_{Et}$ and $\mathbf{7}_{Et}$, or longer hexyl chains in $\mathbf{7}_{Hex}$.

The modification of the molecular structure from **5** to **7** led to a dramatic reduction of the tendency to from a mesophase over unduly large thermal ranges, while the increase of T_g from 19 °C in $\mathbf{5}_{Bu}$ to 39 °C in its core-extended analog $\mathbf{7}_{Bu}$ allowed us to obtain a material that combines a mesomorphic glassy hexagonal columnar state at room temperature with the formation of an isotropic liquid at conveniently attainable temperatures.

We investigated the photophysical properties of **5** and **7** in dilute chloroform solution and in condensed films. In solution the absorption spectra of all homologs of **5** show two main absorption bands (ε = 83 & 113 $mM^{-1}cm^{-1}$) centered at around 342 nm and 272 nm, while the homologs of **7** show a weak absorption (7 $mM^{-1}cm^{-1}$) close to 405 nm, and a combination of intense transitions at high energy, leading to a structured absorption with maxima (62, 65, 95 & 123 $mM^{-1}cm^{-1}$) at 361, 345, 316 and 278 nm (Figure 6). We performed DFT and TD-DFT calculations on optimized geometries of the hexamethyl homologs $\mathbf{5}_{Me}$ and $\mathbf{7}_{Me}$ to gain insights in the configurations of the excited states. For $\mathbf{5}_{Me}$ the low energy band is related to π-π* transitions mostly centered at the triazine core, while the high energy band is also due to π-π* transitions, but mainly spread through the phenanthrene moiety. In $\mathbf{7}_{Me}$ the adopted geometry with less planarity in the tetrahelicenyl moieties leads to a different absorption profile: The low intensity band close to 400 nm arises from a charge-transfer-like state from tetrahelicenyl to triazine. The other transitions are similar to those in **5**, with intermediary energy π-π* states centered at the triazine and those at high energy spread through the tetrahelicenyl moiety.

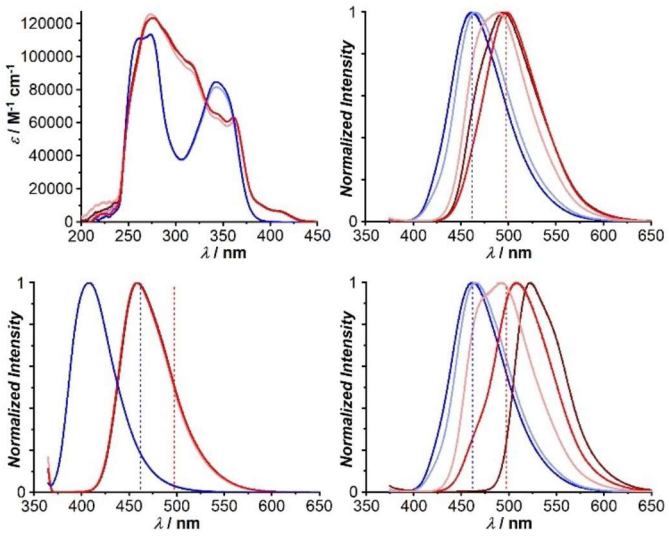

Figure 6. Left: Normalized absorption (top) and emission (bottom) in dilute chloroform solution [10^{-2} mg/mL]. Right: Normalized emission in drop-cast film at room temperature before (top) and after (bottom) heating above the melting point. Emission spectra were obtained upon excitation at 360 nm. $\mathbf{5}_{Pr}$: dark blue, $\mathbf{5}_{Bu}$: light blue, $\mathbf{7}_{Et}$: brown, $\mathbf{7}_{Pr}$: red, $\mathbf{7}_{Bu}$: pink. The dashed lines in the three emission graphs, centered on the emission maxima of $\mathbf{5}_{Pr}$ & $\mathbf{7}_{Pr}$ in unheated films (as shown in the top right graph), are guides to the eye.

The emission in solution shows a single emission peak close to 409 nm for **5** and 458 nm for **7**, with no discernible differences between homologs in either series. From the onset of emission in solution, at ca. 375 nm for **5** and at ca. 420 nm for **7**, energies of the first excited singlet state S_1 of 3.31 eV for **5** and of 2.95 eV for **7** can be inferred. From TD-DFT calculations on optimized geometries of $\mathbf{5}_{Me}$ and $\mathbf{7}_{Me}$, S_1 energies were obtained that are very close to the values inferred from emission in solution: 3.347 eV for $\mathbf{5}_{Me}$ and 2.963 for $\mathbf{7}_{Me}$. We also calculated the energy of the excited triplet states T_1 on the same geometries using SOC-TD-DFT, obtaining 2.637 eV for $\mathbf{5}_{Me}$ and 2.464 eV for $\mathbf{7}_{Me}$. The good correspondence of experimental and DFT-calculated energy values for S_1 indicates that the T_1 energies obtained on the same geometries may be good estimations as well. Materials such as **5** or **7** with T_1 energies of ca. 2.5 eV may accordingly be considered as matrices for TADF emitters that emit light of slightly lower energy, i.e. in the green-to-yellow range of the visible spectrum.

Whereas the absorption spectra and as well as the emission spectra from solution are near-identical between the homologs of **5** and between the homologs of **7**, significant differences between the column-forming homologs of **7** appear in the emission spectra upon annealing of drop-cast films (Figure 6 and Table 2). The emission $\mathbf{5}_{Pr}$, $\mathbf{5}_{Bu}$ and of $\mathbf{7}_{Bu}$, i.e. the three materials that exhibit a conventional hexagonal columnar mesophase in the glassy state at room temperature, is not notably altered upon annealing by melting and subsequent cooling back to room temperature, which suggests that upon solvent evaporation from drop-cast films at room temperature, the same mesogenic state is obtained as upon cooling of the melt. In contrast, the emission spectra of $\mathbf{7}_{Et}$ and $\mathbf{7}_{Pr}$, which adopt respectively a hexagonal crystalline state and a higher-order columnar mesophase at room temperature, shift to the red upon annealing, by 28 nm ($\mathbf{7}_{Et}$) and 11 nm ($\mathbf{7}_{Pr}$). Here the higher order of the polycrystalline film of $\mathbf{7}_{Et}$ and of the highly ordered mesomorphic film of $\mathbf{7}_{Pr}$ is apparently obtained only upon annealing. The bathochromic shift from emission in solution to emission from the columnar mesophase is more pronounced for planar **5** than for distorted **7**, meaning that the flatter core of **5** allows more pronounced chromophore aggregation in the mesophase than the less easily stacking off-planar arene system of **7**.

The photoluminescence quantum yield (PLQY) data show that columnar aggregation tends to increase emission yield (Table 2), as the condensed films show higher PLQYs than the solutions. No significant change of PLQY is observed upon annealing. The increase of yield from solution to columnar film constitutes a peculiar form of aggregation-enhanced emission.[17]

Conclusion

The triphenanthryl-triazine-hexaesters **5** with alkyl ester substituents longer than ethyl, i.e. $\mathbf{5}_{Pr}$ and $\mathbf{5}_{Bu}$, are found to show enantiotropic hexagonal columnar mesophases that can be cooled without crystallization to form a mesomorphic glass. The glass transition temperature is strongly chain-length dependent, with T_g of the shorter propyl homolog $\mathbf{5}_{Pr}$ being about 60 °C higher than the one of $\mathbf{5}_{Bu}$. Thus, a glassy state at and above room temperature can be obtained only with very short alkyl chains, which implies clearing temperatures >375 °C which cannot be reached conveniently. To address this, larger but less planar tris(tetrahelicenyl)-triazine-hexaesters **7** have been designed, which with the same short alkyl chains yield monotropic hexagonal columnar mesophases with conveniently attainable melting and clearing temperatures, and, in the case of $\mathbf{7}_{Bu}$, an improved, i.e. 20 °C higher, glass transition temperature compared to its phenanthryl analog $\mathbf{5}_{Bu}$. The shorter-chain

Table 2. Photoluminescence quantum yields and emission maxima in chloroform solution and in drop-cast film, upon excitation at 360 nm.

	$\mathbf{5}_{Et}$	$\mathbf{5}_{Pr}$	$\mathbf{5}_{Bu}$	$\mathbf{7}_{Et}$	$\mathbf{7}_{Pr}$	$\mathbf{7}_{Bu}$	$\mathbf{7}_{Hex}$
Solution ($CHCl_3$)	22%	21%	22%	12%	12%	12%	12%
	409 nm	407 nm	409 nm	459 nm	458 nm	459 nm	459 nm
Cast film	27%	45%	49%	20%	23%	14%	17%
	462 nm	462 nm	465 nm	495 nm	498 nm	489 nm	500 nm
Annealed film	n/a (does not melt)	44%	46%	24%	23%	13%	16%
		461 nm	466 nm	523 nm	509 nm	493 nm	505 nm

homolog $\mathbf{7}_{Pr}$ shows on cooling, instead of a glass transition, an unusual and intriguing first-order transition to a second hexagonal columnar mesophase with an extremely well-ordered hexagonal column lattice.

The stabilization of a solid-like hexagonal columnar mesophase at room temperature, combined with an accessible transition to the isotropic liquid in order to allow for the formation of surface-aligned samples by cooling from the liquid, is thus shown to be achievable by a molecular design based on configurational flexibility together with a well-dosed intrinsic deviation from planarity and short alkyl ester substituents.

Emission in condensed columnar films at ambient temperature is found to be higher than in solution. The peculiar increase of order of the room temperature mesophase from $\mathbf{7}_{Bu}$ to $\mathbf{7}_{Pr}$ leads to a bathochromic shift of emission in annealed films due to enhanced aggregation.

Acknowledgements

We are grateful to INCT/INEO, CNPq, FAPESC, H2020-MSCA-RISE-2017 (OCTA, #778158), CAPES (Coordenação de aperfeiçoamento de pessoal de nível superior, Brazil. Finance code #937-20 and #001) and COFECUB (Comité français d'évaluation de la coopération universitaire et scientifique avec le Brésil) (joint project Ph-C 962/20) for support. The XRD experiments were carried out in the Laboratório de Difração de Raios X (LDRX/UFSC). FNdS and HML are grateful to the French ministry for Foreign Affairs for Eiffel scholarships.

Conflict of Interest

The authors declare no conflict of interest.

Data Availability Statement

The data that support the findings of this study are available from the corresponding author upon reasonable request.

Keywords: columnar liquid crystal · cyclotrimerization · mesophases · molecular glass · triazine

[1] a) F. Tenopala-Carmona, O. S. Lee, E. Crovini, A. M. Neferu, C. Murawski, Y. Olivier, E. Zysman-Colman, M. C. Gather, *Adv. Mater.* **2021**, *33*, 2100677; b) D. Yokoyama, *J. Mater. Chem.* **2011**, *21*, 19187–19202; c) H. Sasabe, Y. Chikayasu, S. Ohisa, H. Arai, T. Ohsawa, R. Komatsu, Y. Watanabe, D. Yokoyama, J. Kido, *Front. Chem.* **2020**, *8*, 00427.

[2] J. Eccher, G. C. Faria, H. Bock, H. von Seggern, I. H. Bechtold, *ACS Appl. Mater. Interfaces* **2013**, *5*, 11935–11943.

[3] a) T. Woehrle, Tobias I. Wurzbach, J. Kirres, A. Kostidou, N. Kapernaum, J. Litterscheidt, J. C. Haenle, P. Staffeld, A. Baro, F. Giesselmann, S. Laschat, *Chem. Rev.* **2016**, *116*, 1139–1241; b) *Handbook of Liquid Crystals* Vol. 4, 2nd Ed. (Eds: J. W. Goodby, P. J. Collings, T. Kato, C. Tschierske, H. F. Gleeson, P. Raynes), Wiley-VCH, Weinheim, Germany, **1996**; c) *Chemistry of Discotic Liquid Crystals: From Monomers to Polymers* (Ed: S. Kumar), CRC Press, Boca Raton, USA, **2010**.

[4] H. Bisoyi, S. Kumar, *Chem. Soc. Rev.* **2010**, *39*, 264–285.

[5] a) B. Kaafarani, *Chem. Mater.* **2011**, *23*, 378–396; b) S. Sergeyev, W. Pisula, Y. H. Geerts, *Chem. Soc. Rev.* **2007**, *36*, 1902–1929.

[6] a) N. Boden, R. J. Bushby, A. N. Cammidge, A. El-Mansoury, P. S. Martin, Z. Lu, *J. Mater. Chem.* **1999**, *9*, 1391–1402; b) X. Hao, C. Zhang, J. Wang, W. Zhang, F. Hong, S. Zhang, A. Zhang, H. Yang, Z. Zhang, Y. Wang, H. Wu, J. Pu, *J. Mater. Chem. C* **2017**, *5*, 589–600; c) H. Ji, K. Q. Zhao, W. H. Yu, B. Q. Wang, P. Hu, *Sci. China Ser. B* **2009**, *52*, 975–985; d) S. Kumar, M. Manickam, H. Schonherr, *Liq. Cryst.* **1999**, *26*, 1567–1571; e) S. Kumar, *Liq. Cryst.* **2005**, *32*, 1089–1113; f) C. O. Zellman, V. E. Williams, *J. Org. Chem.* **2021**, *86*, 15076–15084.

[7] K. E. Treacher, G. J. Clarkson, N. B. McKeown, *Liq. Cryst.* **1995**, *19*, 887–889.

[8] a) Z. Chen, C. Bishop, E. Thoms, H. Bock, M. D. Ediger, R. Richert, L. Yu, *Chem. Mater.* **2021**, *33*, 4757–4764; b) A. Gujral, J. Gomez, S. Ruan, M. F. Toney, H. Bock, L. Yu, M. D. Ediger, *Chem. Mater.* **2017**, *29*, 9110–9119; c) C. Bishop, Z. Chen, M. F. Toney, H. Bock, L. Yu, M. D. Ediger, *J. Phys. Chem. B* **2021**, *125*, 2761–2770.

[9] a) C.-H. Lee, T. Yamamoto, *Tetrahedron Lett.* **2001**, *42*, 3993–3996; b) H. Lee, D. Kim, H.-K. Lee, W. Qiu, N.-K. Oh, W.-C. Zin, K. Kim, *Tetrahedron Lett.* **2004**, *45*, 1019–1022; c) E. Beltrán, J. L. Serrano, T. Sierra, R. Giménez, *Org. Lett.* **2010**, *12*, 1404–1407; d) E. Beltrán, J. L. Serrano, T. Sierra, R. Giménez, *J. Mater. Chem.* **2012**, *22*, 7797–7805; e) B. N. Veerabhadraswamy, H. K. Dambal, D. S. Shankar Rao, C. V. Yelamaggad, *ChemPhysChem* **2016**, *17*, 1–14; f) B. Pradhan, S. K. Pathak, R. K. Gupta, M. Gupta, S. K. Pal, A. S. Achalkumar, *J. Mater. Chem. C* **2016**, *4*, 6117–6130; g) N. Tober, T. Rieth, M. Lehmann, H. Detert, *Chem. Eur. J.* **2019**, *25*, 15295–15304.

[10] a) A. Pinner, F. Klein, *Chem. Ber.* **1878**, *11*, 764; b) A. H. Cook, D. G. Jones, *J. Chem. Soc.* **1941**, 278.

[11] A. A. Vieira, G. Farias, W. C. Costa, J. Eccher, I. H. Bechtold, F. Durola, H. Bock, *Chem. Eur. J.* **2021**, *27*, 9003–9010.

[12] a) T.-T. Bui, F. Goubard, M. Ibrahim-Ouali, D. Gigmes, F. Dumur, *Beilstein J. Org. Chem.* **2018**, *14*, 282–308; b) C.-L. Yi, C.-L. Ko, T.-C. Yeh, C.-Y. Chen, Y.-S. Chen, D.-G. Chen, P.-T. Chou, W.-Y. Hung, K.-T. Wong, *ACS Appl. Mater. Interfaces* **2020**, *12*, 2724–2732.

[13] L. Sturm, F. Aribot, L. Soliman, H. Bock, F. Durola, *Eur. J. Org. Chem.* **2022**, e202200196.

[14] T. Hassheider, S. A. Benning, H.-S. Kitzerow, M.-F. Achard, H. Bock, *Angew. Chem. Int. Ed.* **2001**, *40*, 2060–2063; *Angew. Chem.* **2001**, *113*, 2119–2122.

[15] A. M. Levelut, *J. Chim. Phys.* **1983**, *80*, 149–61.

[16] L. Zhao, R. I. Kaiser, B. Xu, U. Ablikim, W. Lu, M. Ahmed, M. M. Evseev, E. K. Bashkirov, V. N. Azyazov, M. V. Zagidullin, A. N. Morozov, A. H. Howlader, S. F. Wnuk, A. M. Mebel, D. Joshi, G. Veber, F. R. Fischer, *Nat. Commun.* **2019**, *10*, 1510.

[17] B. Liu, B. Z. Tang, *Angew. Chem. Int. Ed.* **2020**, *59*, 9788–9789; *Angew. Chem.* **2020**, *132*, 9872–9873.